

New Developments in Axion Cosmology

(And Some Old Ones)

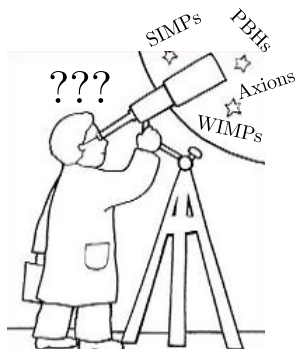
Joshua Eby

Weizmann Institute of Science
Rehovot, Israel

March 20, 2018

Theory Seminar, Fermi National Accelerator Laboratory

Dark Matter



To reproduce:

- Rotation curves
- Relic density
- Stable; Early universe production

To distinguish:

- Cosmological history
- Interactions with SM
- Small-Scale Structure

Axions

Largest scales:

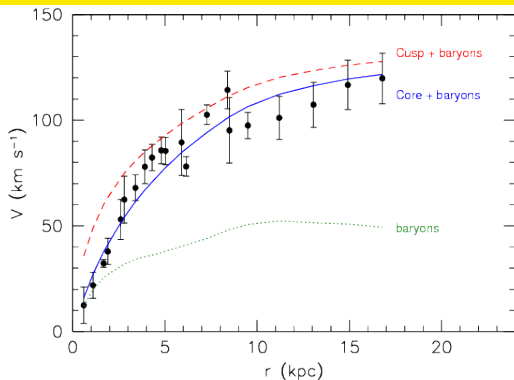
- ✓ Pressureless
- ✓ Stable; Relic density
- ✓ Early universe

(Just like every other DM model)

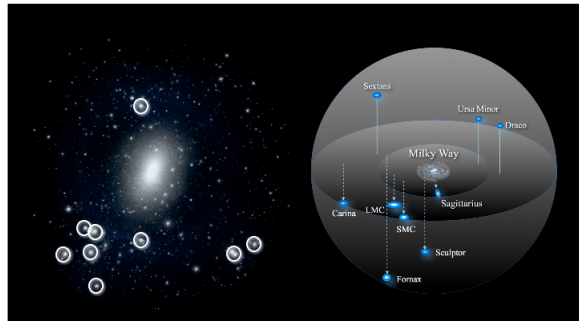
Unique features

- History:
 - Interactions at high scales
 - Thermal / Relativistic production
 - Domain walls
- Interactions:
 - Direct Axion Detection (ADMX, etc.)
- Small Scale Structure:
 - **This talk**

Dark Matter at Small Scales



- Signs of self-interactions?
- Nontrivial dark sector?
- **Dark matter structures matter**



[Weinberg et al., 1306.0913]

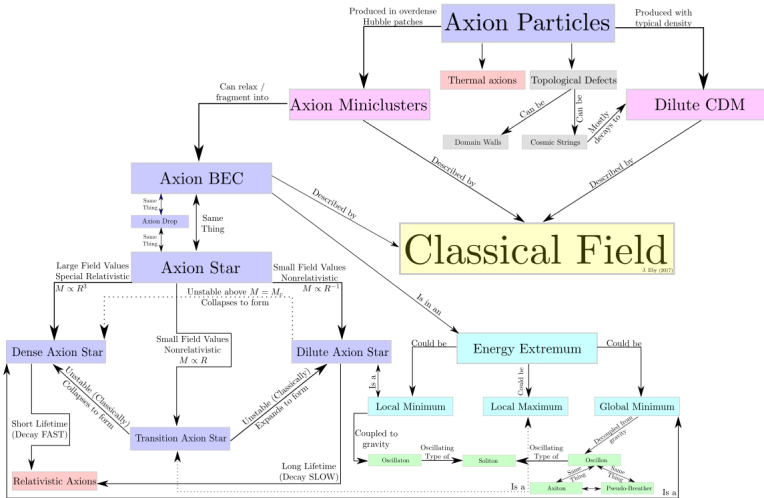
Take Home Message

In this talk, focus on axion dark matter.

- Axions are still extremely well-motivated DM candidate
- Natural parameter space unconstrained
- Highly nontrivial substructure at sub-galaxy distance scales

Small scale structure \Leftrightarrow Large density fluctuations (of asteroid, planet, star sizes)

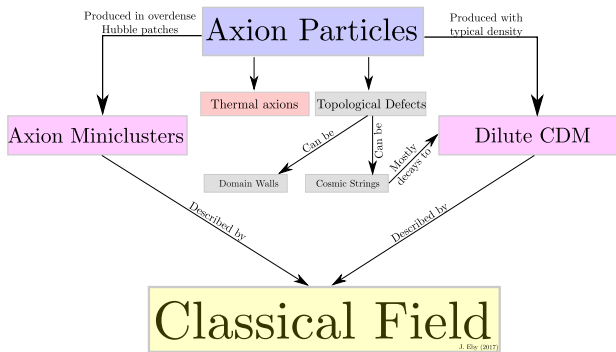
Quick Review



Outline

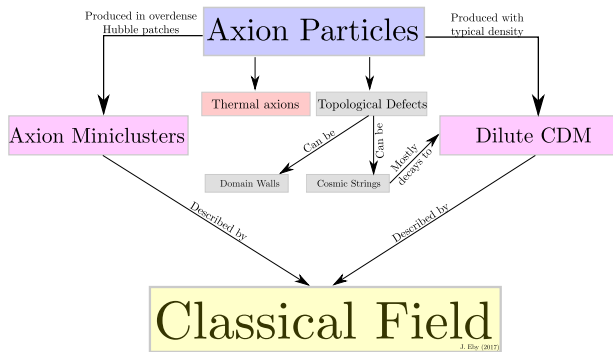
- Axion / Dark Matter Fundamentals (Zooming out)
- Small-Scale Structure in Axion Cosmology (Zooming in again)
 - Axion miniclusters
 - Axion stars
 - Dense axion stars
- Conclusions

Axion Cosmology on Largest Scales



- Production: (1) Classical field (2) Topological defects (3) Thermal component

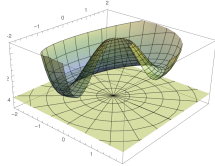
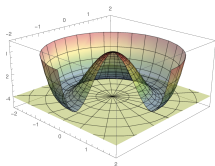
Axion Cosmology on Largest Scales



- Production: (1) Classical field (2) Topological defects (3) Thermal component

Axion Field History

1. $U(1)_{PQ}$ symmetry broken at scale f
2. Massless NGB, **axion**, $a(x) = f \theta(x)$
3. Potential tilted at Λ ; mass $m = \frac{\Lambda^2}{f} \neq 0$
4. Oscillations commence at T_{osc}



QCD axion:

3a. Tilt: $\Lambda = \Lambda_{QCD}$

4a. Oscillations: $T_{osc} \simeq \Lambda_{QCD}$

Axion-like particle (ALP)

3b. Tilt: Λ free

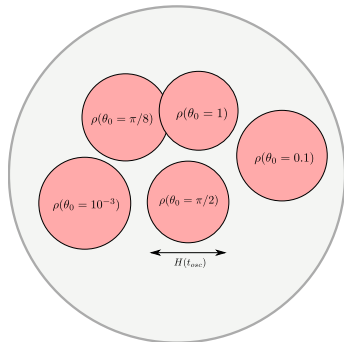
4b. Oscillations: $3H(T_{osc}) \simeq m(T_{osc})$

5. Relic density related to misalignment angle θ_0

Low-energy potential: $V(\theta) = m^2 f^2 (1 - \cos \theta)$

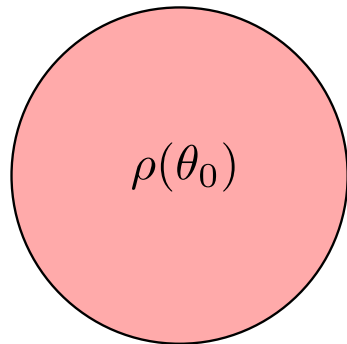
Phase Transition

Case 1: f below inflation scale



$$\Omega_{a,0} \equiv \frac{\rho_{a,0}}{\rho_c} \sim \left(\frac{f}{10^{12} \text{ GeV}} \right)^{7/6} \langle \theta_0^2 \rangle$$

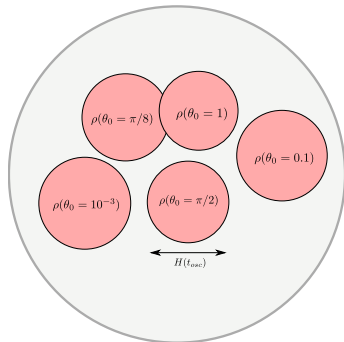
Case 2: f above inflation scale



$$\Omega_{a,0} \equiv \frac{\rho_{a,0}}{\rho_c} \sim \left(\frac{f}{10^{12} \text{ GeV}} \right)^{7/6} \theta_0^2$$

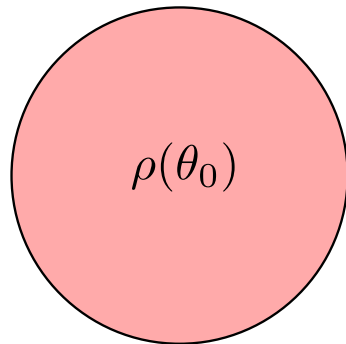
Phase Transition

Case 1: f below inflation scale



$$\Omega_{a,0} \equiv \frac{\rho_{a,0}}{\rho_c} \sim \left(\frac{f}{10^{12} \text{ GeV}} \right)^{7/6} \langle \theta_0^2 \rangle$$

Case 2: f above inflation scale



$$\Omega_{a,0} \equiv \frac{\rho_{a,0}}{\rho_c} \sim \left(\frac{f}{10^{12} \text{ GeV}} \right)^{7/6} \theta_0^2$$

Zoom In (x1)



Density Contrasts

Large distance scales: Expand potential $V(\theta) = m^2 f^2 (1 - \cos \theta) \approx \frac{m^2 f^2}{2} \theta^2$

Small Fluctuations:

- Different patches choose $\theta_0 \in [0, \pi]$

$$\frac{\delta\rho}{\bar{\rho}} = \frac{m^2 f^2 \sqrt{\langle\theta_0^2\rangle} \delta\theta}{\frac{1}{2} m^2 f^2 \langle\theta_0^2\rangle} \sim \frac{2\delta\theta}{\theta_0} \sim [0, 2]$$

- Overdensities: “Axion Miniclusters”

[Hogan and Rees, 1988]

And larger ones:

[Fairbairn et al., 1707.03310]

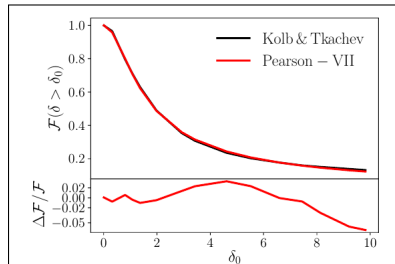


FIG. 2. **Minicluster Overdensity Distribution:** We show the cumulative mass fraction of miniclusters with overdensity parameter $\delta > \delta_0$. The black line shows the simulation results of Ref. [22], which we have fit using a Pearson-VII distribution. The overdensity distribution determines the halo concentration parameter (i.e. compactness) of miniclusters.

Minicluster Properties

$$\text{At } \Lambda_{\text{QCD}}, \rho_a = (1 + \Phi)\bar{\rho}$$

[Kolb and Tkachev astro-ph/9311037]

$$\rightarrow \rho_{mc} \approx 140\Phi^3(1 + \Phi)\bar{\rho}(T_{eq}) \approx 3 \times 10^{-14} \frac{\text{g}}{\text{cm}^3} \Phi^3(1 + \Phi)$$

$$R \sim \frac{2 \times 10^6 \text{ km}}{\Phi(1 + \Phi)^{1/3}} \left(\frac{M}{10^{-12} M_\odot} \right)^{1/3}$$

Minicluster Properties

At Λ_{QCD} , $\rho_a = (1 + \Phi)\bar{\rho}$

[Kolb and Tkachev astro-ph/9311037]

$$\rightarrow \rho_{mc} \approx 140\Phi^3(1 + \Phi)\bar{\rho}(T_{eq}) \approx 3 \times 10^{-14} \frac{\text{g}}{\text{cm}^3} \Phi^3(1 + \Phi)$$

$$R \sim \frac{2 \times 10^6 \text{ km}}{\Phi(1 + \Phi)^{1/3}} \left(\frac{M}{10^{-12} M_\odot} \right)^{1/3}$$

Huge occupation number: today, for $\rho_{DM} = 0.4 \frac{\text{GeV}}{\text{cm}^3}$,

$$\mathcal{N} \sim \frac{\rho_{DM}}{m^4 \delta V^3} \sim 10^{26} \quad (\text{virialized axion with } m \sim 10^{-5} \text{ eV})$$

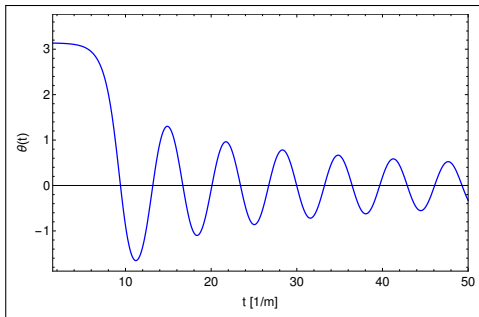
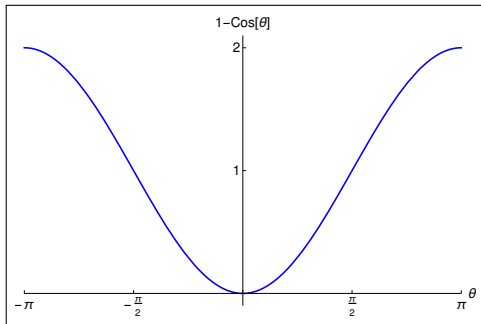
Early times: classical field in expanding universe,

$$\ddot{\theta} - \nabla^2 \theta + 3H\dot{\theta} + m^2 \sin \theta = 0$$

Late times: classical field coupled to gravity,

$$i\dot{\psi} = -\frac{1}{2m} \nabla^2 \psi + V_g \psi + V_{int} \psi$$

Anharmonic Effects

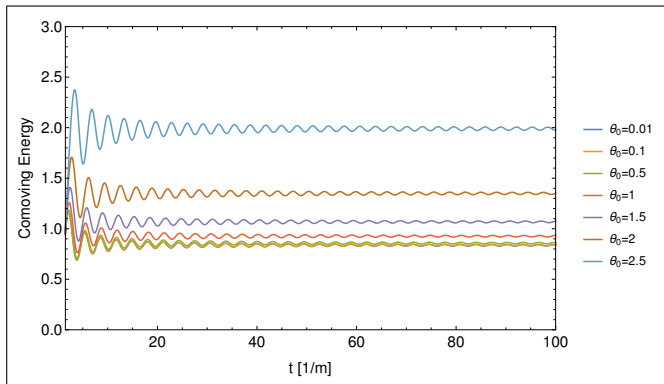


$$\ddot{\theta} - \nabla^2\theta + 3H\dot{\theta} + m^2 \sin\theta = 0$$

Increasing Density

Start from $\theta = \theta_0$ at $t = t_{osc}$, evolve until oscillations stabilize

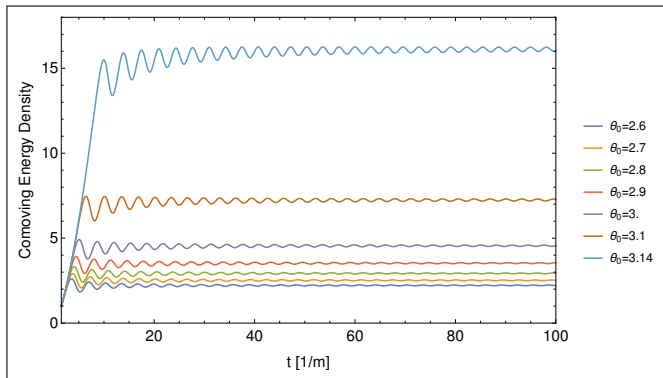
$$\ddot{\theta} + 3H\dot{\theta} + m^2 \sin \theta = 0$$



Increasing Density

Start from $\theta = \theta_0$ at $t = t_{osc}$, evolve until oscillations stabilize

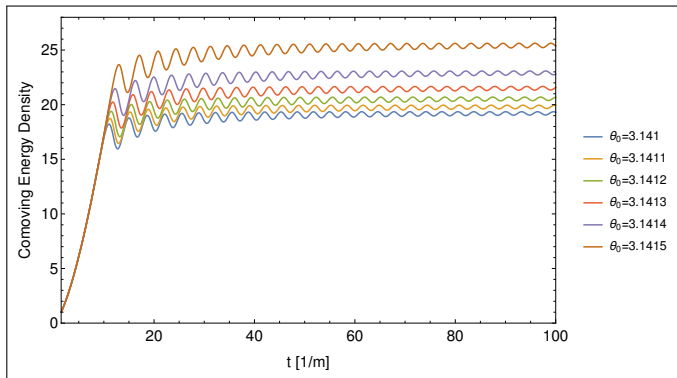
$$\ddot{\theta} + 3H\dot{\theta} + m^2 \sin \theta = 0$$



Increasing Density

Start from $\theta = \theta_0$ at $t = t_{osc}$, evolve until oscillations stabilize

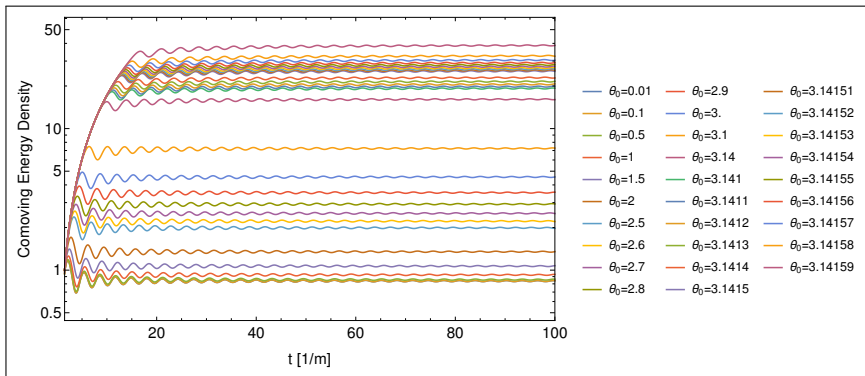
$$\ddot{\theta} + 3H\dot{\theta} + m^2 \sin \theta = 0$$



Increasing Density

Start from $\theta = \theta_0$ at $t = t_{osc}$, evolve until oscillations stabilize

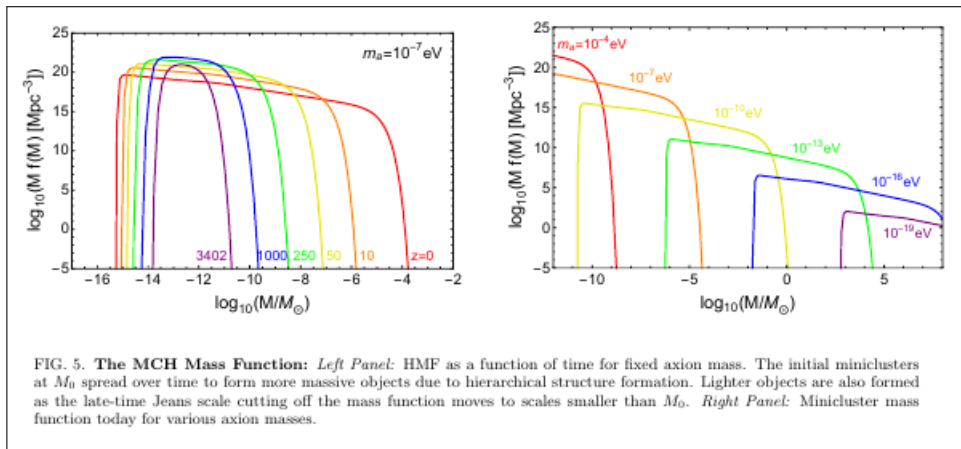
$$\ddot{\theta} + 3H\dot{\theta} + m^2 \sin \theta = 0$$



Minicluster Mass

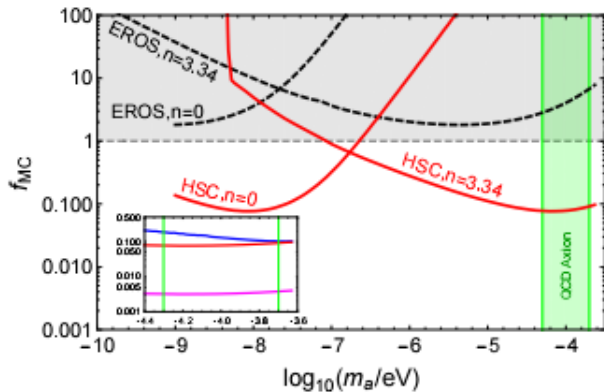
Large Density Contrasts!

[Fairbairn et al., 1707.03310]



Lensing Constraints

[Fairbairn et al. 1707.03310]



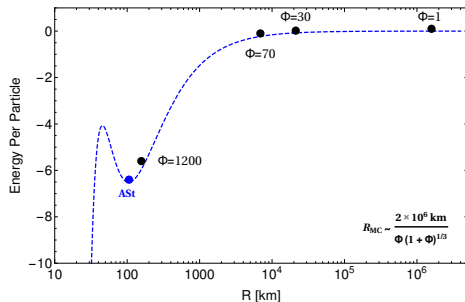
Minicluster Radius

Different question: At fixed M_{MC} , how does density evolve?

$$\frac{E[\psi]}{N} = \frac{1}{N} \int d^3r K[\psi] + W[\psi] + V_{int}[\psi]$$

Recall overdensity $\rho = (1 + \Phi)\bar{\rho}$:

For $\Phi \gtrsim 30$, $t_{relaxation} < \text{age of Universe}$ to form "axion star", ground state of the system



Zoom In (x2)

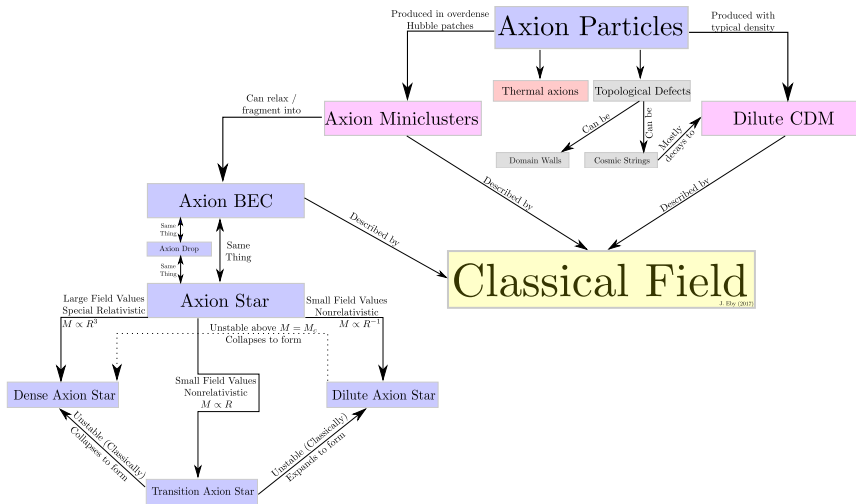


Axion Miniclusters \neq Axion Stars

- Minicluster size / mass determined by **cosmological factors** : DM density at z_{QCD} , Hubble size, etc.
 - Axion star size / mass determined by **ground state configuration** of classical equation of motion
- ! No reason to suppose these are the same!

Even if $f_{ASt} \sim 1\%$ component of dark matter, can have huge impact!

Axion Stars



Axion Stars

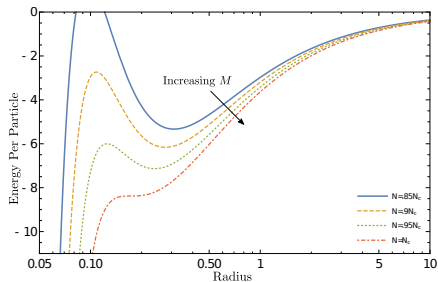
In axion star, leading self-interaction $-\lambda \phi^4$ important

- Energy has local minimum
- Mass/Radius relation $M \propto \frac{1}{R}$
- Maximum mass

$$M_c \simeq \left(\frac{f}{6 \times 10^{11} \text{ GeV}} \right) \left(\frac{10^{-5} \text{ eV}}{m} \right) 10^{-11} M_\odot$$

- Minimum radius

$$R_c \simeq \left(\frac{6 \times 10^{11} \text{ GeV}}{f} \right) \left(\frac{10^{-5} \text{ eV}}{m} \right) 200 \text{ km}$$



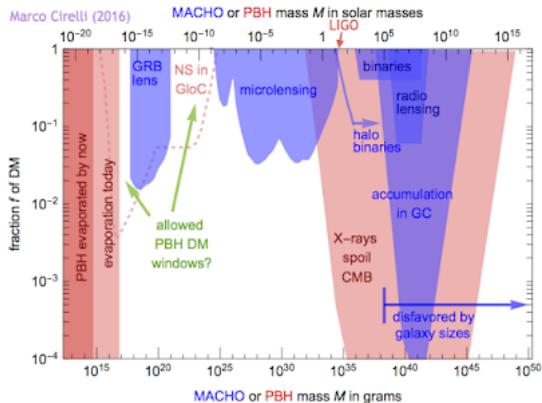
[JE, Leembruggen, Suranyi, Wijewardhana
1608.06911]

Lensing from Axion Stars

Axion stars are denser than miniclusters, but weakly constrained by lensing

$$M_c \simeq \left(\frac{f}{6 \times 10^{11} \text{ GeV}} \right) \left(\frac{10^{-5} \text{ eV}}{m} \right) 10^{-11} M_\odot$$

$$R_c \simeq \left(\frac{6 \times 10^{11} \text{ GeV}}{f} \right) \left(\frac{10^{-5} \text{ eV}}{m} \right) 200 \text{ km}$$



Collision Rate

Collisions with Earth are (usually) pretty rare

[JE et al., 1701.01476]

- Number

$$N_{ASt} \simeq \frac{\mathcal{F}_{DM} M_{DM}}{M_{ASt,0}} \simeq \mathcal{F}_{DM} \times 10^{23} \times \left(\frac{10^{-11} M_{\odot}}{M_{ASt,0}} \right)$$

- Cross section

$$\sigma_i = \pi (R_{ASt} + R_i)^2 \left(1 + \frac{v_{esc}^2}{v^2} \right)$$

→ Rate

$$\Gamma_i \simeq N_{ASt} \sigma_i \frac{N_i v}{V_{galaxy}}$$

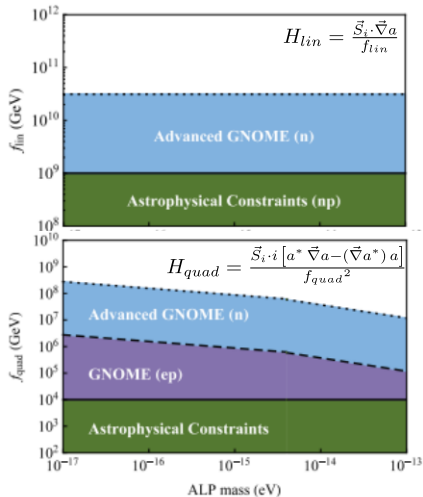
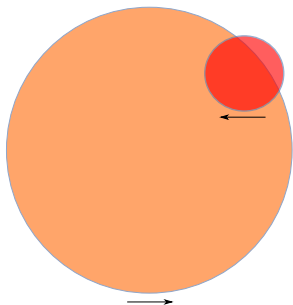
If you want $\mathcal{O}(1/\text{year})$, require

$$10 R_E \lesssim R_{ASt} \lesssim 10^6 R_E, \quad M \lesssim 10^{-16} M_{\odot}$$

Axion Star Collisions

- In collision with earth, $\rho_{DM} \rightarrow \rho_{DM}(t)$!
- In any one detector, see a large 'blip'
- Time-correlated detectors:
Global Network of Optical Magnetometer to search for Exotic physics (GNOME)

[Kimball, JE, et al., 1710.04323]

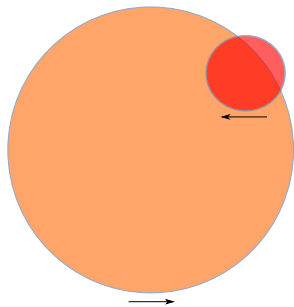


Other Collisions: Ordinary Stars

$$N_{\odot} \gg N_{\text{Earths!}}$$

[JE et al., 1701.01476]

- Additional gravity can decrease $M_c \Rightarrow$ collapse
- For QCD, typically $R_s \gg R_{AS}$
- $\Gamma \sim 3000 \mathcal{F}_{DM} \frac{\text{collisions}}{\text{year} \cdot \text{galaxy}}$

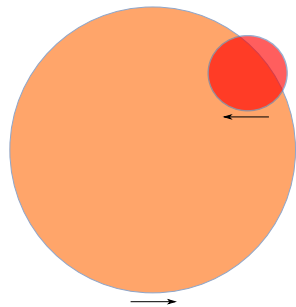
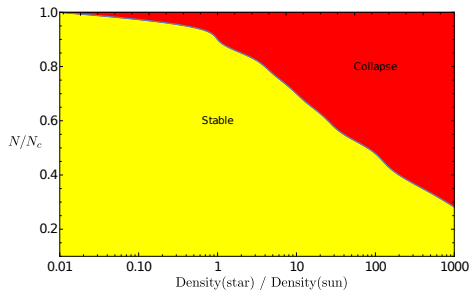


Other Collisions: Ordinary Stars

$$N_{\odot} \gg N_{\text{Earths!}}$$

[JE et al., 1701.01476]

- Additional gravity can decrease $M_c \Rightarrow$ collapse
- For QCD, typically $R_s \gg R_{AS}$
- $\Gamma \sim 3000 \mathcal{F}_{DM} \frac{\text{collisions}}{\text{year} \cdot \text{galaxy}}$



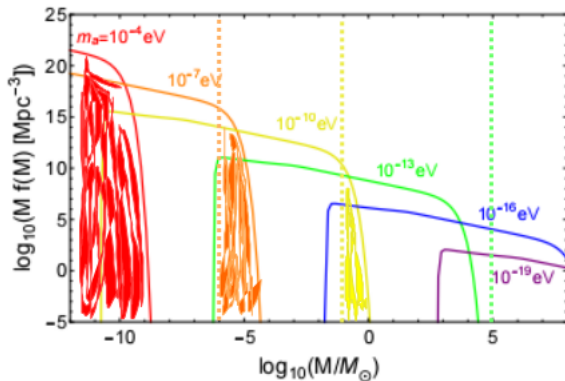
- Depends stellar density \mathcal{D}
- Nearly all collisions near M_c cause collapse

Zoom In (x3)



Some Miniclusters Too Heavy

Some $M_{MC} > M_{c, Ast}$. Then what do they collapse to?



[Adapted from Fairbairn et al. 1707.03310]

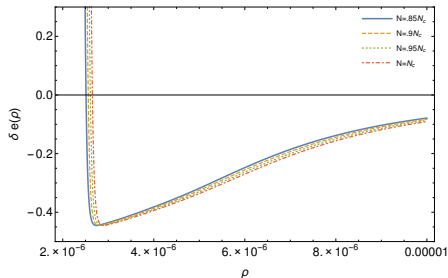
Dense Axion Stars

[JE, Leembruggen, Suranyi, Wijewardhana 1608.06911]

Above M_c , collapse

- $R \rightarrow 0$ corresponds to $\phi \rightarrow f$ or $\theta \rightarrow \pi$
- Can't just truncate at ϕ^4
- Short range **repulsive** int's at small R ,
classically stable **dense axion stars**

[Braaten et al., 1512.00108]



Relativistic Contributions

Dense axion stars have large binding energies $\Rightarrow m \simeq E \Rightarrow$ SR corrections

- Kinetic energy:

$$-\frac{\nabla^2}{2m} \rightarrow \sqrt{1 - \frac{\nabla^2}{m^2}} - m$$

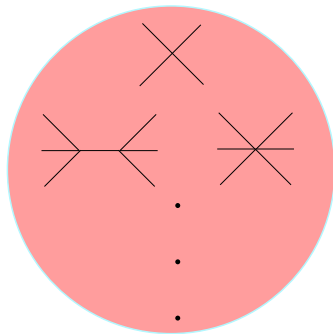
[Guth et al., 1712.00445]

- Self-interaction:

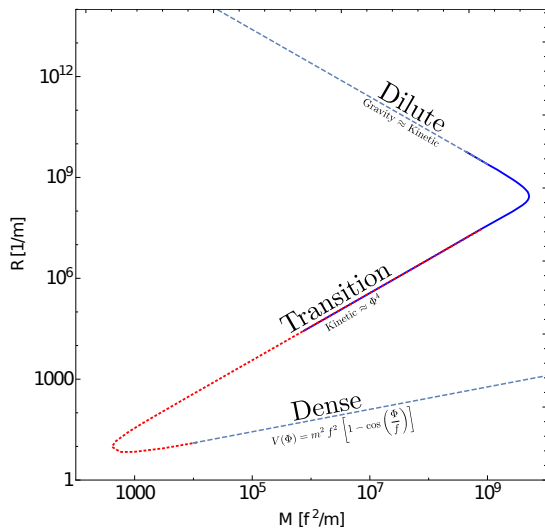
$$\begin{aligned} V(\theta) &= m^2 f^2 (1 - \cos \theta) \\ &\approx \frac{m^2 f^2}{2} \theta^2 - \frac{m^2 f^2}{4!} \theta^4 + \frac{m^2 f^2}{6!} \theta^6 - \dots \end{aligned}$$

- Higher mode expansion: $E, 3E, 5E, \dots$

[JE, Suranyi, and Wijewardhana, 1712.04941]



Mass Distribution of Axion Stars



Ongoing: The NR Limit

Standard procedure: $\ddot{\phi} - \nabla^2 \phi - \frac{\lambda}{3!} \phi^3 \rightarrow i\dot{\psi} = -\frac{1}{2m} \nabla^2 \psi - \frac{\lambda}{8m^2} |\psi|^2 \psi$ with

$$\phi = \frac{1}{\sqrt{2m}} [e^{-imt} \psi + e^{imt} \psi^*]$$

How do we organize corrections?

Ongoing: The NR Limit

Standard procedure: $\ddot{\phi} - \nabla^2 \phi - \frac{\lambda}{3!} \phi^3 \rightarrow i\dot{\psi} = -\frac{1}{2m} \nabla^2 \psi - \frac{\lambda}{8m^2} |\psi|^2 \psi$ with

$$\phi = \frac{1}{\sqrt{2m}} [e^{-imt} \psi + e^{imt} \psi^*]$$

How do we organize corrections?

[Mukaida, Takimoto, Yamada, 1612.07750]

Modes of ϕ :

$$\phi = \frac{1}{\sqrt{2m}} \sum_{\nu=1}^{\infty} [e^{-i\nu mt} \psi_{\nu} + h.c.]$$

Effective interaction $+\frac{\lambda^2}{2304m^5} |\psi_1|^4 \psi_1$

[Namjoo, Guth, Kaiser, 1712.00445]

Modes of ψ :

$$\psi = \sum_{\nu=-\infty}^{\infty} e^{i\nu mt} \psi_{\nu}$$

Effective interaction $-\frac{17\lambda^2}{768m^5} |\psi_0|^4 \psi_0$

As we know...

” All things that have form eventually
decay “ -Orochimaru

As we know...

” All things that have form eventually
decay “ -Orochimaru

(If they have no symmetry protecting number conservation)

Decay: End of the Story

Axions: **No number conservation**

Leading decay rate depends on choice of EFT?

" ϕ -EFT" \rightarrow [JE, Suranyi, Wijewardhana,
1512.01709, 1705.05385]

- $3 a_c \rightarrow a_f$ dominates
- Rate $\Gamma \propto m \exp -(E_B/m)^{-2}$

" ψ -EFT" \rightarrow [Braaten, Mohopatra, Zhang,
1609.05182]

- Particles on-shell, no $3a \rightarrow a$
- Dominant rate $4a \rightarrow 2a$ suppressed

But: Dense axion star = "Sine-Gordon Oscillon", known classical lifetime

[Wilczek et al., 1710.08910]

$$\tau \sim \left(\frac{10^{-5} \text{ eV}}{m} \right) 10^{-7} \text{ sec}$$

Seems like dense axion stars decay extremely fast, but there may be more to the story

Conclusions

Zooming in to small-scale axion structures, tells an interesting story:

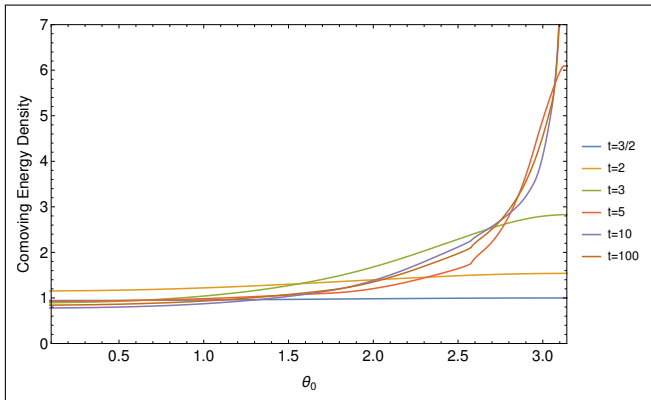
- **Dilute background** with average density $\Omega_a = \frac{\bar{\rho}_a}{\rho_c} \sim \left(\frac{f}{10^{12} \text{ GeV}} \right)^{7/6} \langle \theta_0^2 \rangle$
- **Miniclusters** of "typical" density $\rho_{mc} \sim 200 \bar{\rho}_a$
- Unusually dense miniclusters relax fast, others may fragment, towards the ground state of the system, **dilute axion stars**, of typical density $\rho_{ASt} \sim 10^{10} \rho_{mc}$
- Above a critical mass, can collapse further towards **dense axion stars** of typical density $\rho_{dense} \sim 10^{18} \rho_{ASt}$
- The finale: Dense axion stars seem to decay very quickly to **relativistic axions!**
(Need to understand process better)

Each of these is a unique handle for understanding **axion dark matter** !

Backup Slides

Comoving Energy

$$\ddot{\theta} - 3H\dot{\theta} + m^2 \sin \theta = 0$$



MC Phenomenology

- Femtolensing and Picolensing
- Microlensing

[Kolb and Tkachev astro-ph/9510043]

[Fairbairn et al. 1707.03310]

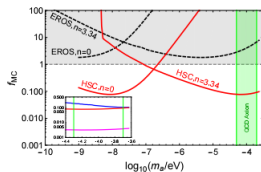


FIG. 16. Limits on the Fraction of DM collapsed into Miniclusters: The model adopted is for “isolated miniclusters”, which we consider the most realistic. The shaded region shows the allowed mass for the QCD axion with miniclusters. Where the $n = 3.34$ lines intersect this region, f_{MC} is constrained for the QCD axion. The inset shows a zoom-in. The magenta (blue) line in the inset shows a hypothetical improved observation by HSC ten nights with an efficiency $\epsilon \sim 1$ in the case of isolated miniclusters (dense MHCs).

MC Phenomenology

- Femtolensing and Picolensing
- Microlensing
- ...though could be affected by minicluster destruction

[Kolb and Tkachev astro-ph/9510043]

[Fairbairn et al. 1707.03310]

[Tkachev et al. 1710.09586]

Important for "direct detection" axion experiments:

- If axions are exceedingly "clumpy", we might have to wait for a collision with axion "clump"
- "Clumpier" \rightarrow Lower collision rate
- Alternative: The Global Network of Optical Magnetometers to search for Exotic physics (GNOME) [Kimball et al. 1710.04323]

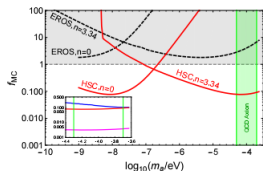


FIG. 16. Limits on the Fraction of DM collapsed into Miniclusters: The model adopted is for "isolated miniclusters", which we consider the most realistic. The shaded region shows the allowed mass for the QCD axion with miniclusters. Where the $n = 3.34$ lines intersect this region, f_{MC} is constrained for the QCD axion. The inset shows a zoom-in. The magenta (blue) line in the inset shows a hypothetical improved observation by HSC ten nights with an efficiency $\epsilon \sim 1$ in the case of isolated miniclusters (dense MHCs).

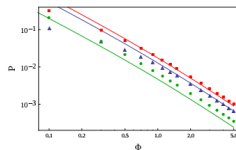


Figure 17. Fraction of destroyed axion miniclusters during their interactions with disk stars versus density perturbation Φ for the Galactic halo with the Navarro-Frenk-White density profile. The circles indicate the result of our calculation using Eq. (25), while the solid line indicates the approximate expression (38). The triangles indicate the result of our exact calculation using Eq. (32), while the corresponding solid line indicates the approximate expression (39). The total fraction of destroyed axion miniclusters is indicated by the squares, while the solid line passing through them indicates the sum of (38) and (39).

Variational Method: Minimize Axion Star Energy

Self-interaction energy of an ASt, in the non-relativistic limit:

$$W(\psi) = -m^2 f^2 \sum_{k=0}^{\infty} (-1)^k a_k \left[\frac{\psi^* \psi}{2 m f^2} \right]^{k+2}$$

The total energy

$$E(\psi) = \int d^3 r \left[\overbrace{\frac{|\nabla \psi|^2}{2m}}^{\text{kinetic}} + \overbrace{\frac{1}{2} V_{\text{grav}}(|\psi|^2)}^{\text{gravitational}} + \overbrace{W(\psi)}^{\text{self-interaction}} \right]$$

We make an ansatz for the wavefunction $\psi(r)$ and compute E :

Rescale: Energy e , Radius ρ , and Particle number n

$$e(\rho) \equiv \frac{E(\rho)}{m N \delta} = \frac{\alpha}{\rho^2} - \frac{\beta n}{\rho} - \frac{1}{\delta} \sum_{k=0}^{\infty} (-1)^k \gamma_k \left(\frac{n \delta}{\rho^3} \right)^{k+1}$$

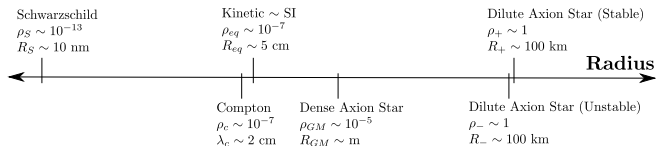
$$\delta \equiv f^2 / M_P^2 \ll 1 \quad \alpha, \beta, \gamma_k \text{ ansatz-dependent constants}$$

Minima of E w.r.t. ρ are stable bound states, axion stars!

Collapse of Dilute ASts

A dilute ASt can collapse if e.g. its mass exceeds M_c . Variational approximation of the total energy $E(\rho)$ lends itself directly to a classical collapse analysis:¹

- LO: Collapse to black hole.
- Full axion potential: Collapse from dilute to dense ASt state!



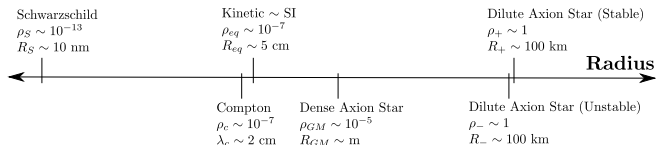
¹Leading Order: Chavanis (1604.05904); Full axion potential: (1608.06911)

²(1512.01709); Braaten/Mohopatra/Zhang (1609.05182); Mukaida/Takimoto/Yamada (1612.07750)

Collapse of Dilute ASts

A dilute ASt can collapse if e.g. its mass exceeds M_c . Variational approximation of the total energy $E(\rho)$ lends itself directly to a classical collapse analysis:¹

- LO: Collapse to black hole.
- Full axion potential: Collapse from dilute to dense ASt state!



However: Possible quantum mechanical effects lead to decay of ASts.

Axions are **real scalars** \Rightarrow No symmetry protects axion number

- Can decay through $a \rightarrow 2\gamma$ (in free or condensed state)
- Inside the condensate, novel decay mechanisms are allowed through self-interactions:²
 - Microscopic picture: $N a_c \rightarrow N' a_c + j a_f$
 - Macroscopic picture: $\mathcal{A}_N \rightarrow \mathcal{A}_{N'} + j a_f$

Leading order process: Emission of single relativistic axion, momentum $p = \sqrt{9 E_0^2 - m^2} \approx \sqrt{8} m$

¹Leading Order: Chavanis (1604.05904); Full axion potential: (1608.06911)

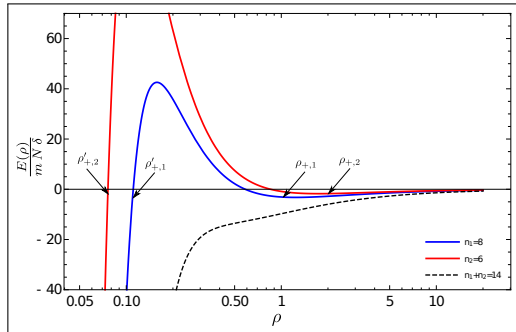
²(1512.01709); Braaten/Mohopatra/Zhang (1609.05182); Mukaida/Takimoto/Yamada (1612.07750)

Collisions: 2 Axion Stars

Energy functional changes to

$$\frac{E_{2AS}}{m(N_1 + N_2)\delta} = \frac{\alpha}{\rho^2} - \frac{\beta(n_1 + n_2)}{\rho} - \frac{\gamma_0(n_1 + n_2)}{\rho^3} + \dots$$

If $N_1 + N_2 > N_c$, collapse!



Collisions: 2 Axion Stars

Energy functional changes to

$$\frac{E_{2AS}}{m(N_1 + N_2)\delta} = \frac{\alpha}{\rho^2} - \frac{\beta(n_1 + n_2)}{\rho} - \frac{\gamma_0(n_1 + n_2)}{\rho^3} + \dots$$

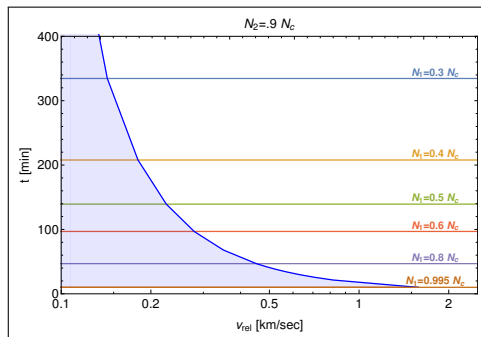
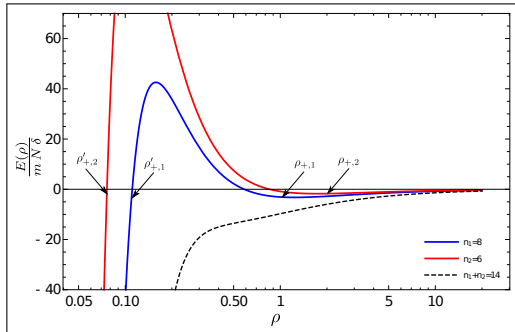
If $N_1 + N_2 > N_c$, collapse!

Long time for collapse to be completed:

$$\text{Total } \Gamma \sim 10^7 \left(\frac{\mathcal{F}_{DM}}{\mathcal{F}_{AS}} \right)^2 \frac{\text{collisions}}{\text{year} \cdot \text{galaxy}}$$

$$\text{But } P(v_{rel} \lesssim 1 \text{ km/sec}) \sim 10^{-8}$$

⇒ Small total collapse rate



Relativistic Classical Field Analysis

This is the framework used by Kaup (for $\Lambda = 0$) and by Colpi et al. (for $\Lambda \gg 1$):

$$\begin{aligned}\frac{A'}{A^2 x} + \frac{1}{x^2} \left(1 - \frac{1}{A}\right) &= \left(\frac{\Omega^2}{B} + 1\right) \sigma^2 + \frac{\Lambda}{2} \sigma^4 + \frac{(\sigma')^2}{A} \\ \frac{B'}{B^2 x} + \frac{1}{x^2} \left(1 - \frac{1}{A}\right) &= \left(\frac{\Omega^2}{B} + 1\right) \sigma^2 - \frac{\Lambda}{2} \sigma^4 + \frac{(\sigma')^2}{A} \\ \sigma'' + \left(\frac{2}{x} + \frac{B'}{2B} - \frac{A'}{2A}\right) \sigma' + A \left[\left(\frac{\Omega^2}{B} - 1\right) \sigma - \Lambda \sigma^3 \right] &= 0,\end{aligned}$$

where the rescaled variables are $x = m r$, $\sigma = \sqrt{4\pi G} \phi$, $\Omega = \mu_0/m$ (μ_0 the eigenenergy of one boson), and $\Lambda = \lambda M_P^2 / (4\pi m^2)$

- Kaup: Non interacting theories have $M_{max}^{NI} = .633 \frac{M_P^2}{m}$
- Colpi et al.: Repulsively interacting theories have $M_{max}^{rep} = .22 \sqrt{\frac{\lambda}{4\pi}} \frac{M_P^3}{m^2}$

RB for Axions

Expectation values of EKG:

$$\begin{aligned}\langle N | G_{\mu}^{\nu} | N \rangle &= 8 \pi G \langle N | T_{\mu}^{\nu} | N \rangle \\ \langle N - 1 | [\mathcal{D} \mathcal{A} - V'(\mathcal{A})] | N \rangle &= 0\end{aligned}$$

The resulting equations of motion take the form

$$\begin{aligned}\frac{A'}{A^2 r} + \frac{A-1}{A r^2} &= \frac{8 \pi f^2}{M_P^2} \left[\frac{\mu_0^2 N R^2}{B f^2} + \frac{N R'^2}{A f^2} + m^2 \left[1 - J_0 \left(\frac{2\sqrt{N} R}{f} \right) \right] \right], \\ \frac{B'}{A B r} - \frac{A-1}{A r^2} &= \frac{8 \pi f^2}{M_P^2} \left[\frac{\mu_0^2 N R^2}{B f^2} + \frac{N R'^2}{A f^2} - m^2 \left[1 - J_0 \left(\frac{2\sqrt{N} R}{f} \right) \right] \right], \\ \sqrt{N} R'' + \sqrt{N} \left(\frac{2}{r} + \frac{B'}{2B} - \frac{A'}{2A} \right) R' + A \left[\frac{\sqrt{N} \mu_0^2}{B} R - f m^2 J_1 \left(\frac{2\sqrt{N} R}{f} \right) \right] &= 0\end{aligned}$$

RB for Axions (2)

Metric functions:

$$A = 1 + \delta a, \quad B = 1 + \delta b$$

EKG at leading order in $\delta = 8\pi f^2/M_P^2$:

$$a' = -\frac{a}{z} + z \left[\frac{1}{4} \epsilon_\mu^2 Z^2 + \frac{1}{4} Z'^2 + 1 - J_0(Z) \right],$$

$$b' = \frac{a}{z} + z \left[\frac{1}{4} \epsilon_\mu^2 Z^2 + \frac{1}{4} Z'^2 - 1 + J_0(Z) \right],$$

$$Z'' = \left[-\frac{2}{z} + \frac{\delta}{2} (a' - b') \right] Z' - \epsilon_\mu^2 (1 + \delta a - \delta b) Z + 2(1 + \delta a) J_1(Z)$$

RB for Axions (3)

EKG at leading order in δ and $\Delta = \sqrt{1 - \epsilon_\mu^2}$:

$$a'(x) = \frac{x}{2} Y(x)^2 - \frac{a(x)}{x},$$

$$b'(x) = \frac{a(x)}{x},$$

$$Y''(x) = -\frac{2}{x} Y'(x) - \frac{1}{8} Y(x)^3 + [1 + \kappa b(x)] Y(x)$$

Particle Number in Real Scalar Field Theory

Recall that the conjugate momentum for a scalar field Φ can be written as

$$\Pi = D_t \Phi = \frac{1}{B} \left[-i \mu_n R_n(\vec{r}) e^{-i \mu_n t} a_n + i \mu_n R_n^\dagger(\vec{r}) e^{i \mu_n t} a_n^\dagger \right],$$

which is implicitly summed over n . D_t is a covariant time derivative which gives rise to the metric function B in the denominator. Then

$$[\Phi(\vec{r}), \Pi(\vec{r}')] = \frac{2}{B} R_n^\dagger(\vec{r}) R_n(\vec{r}').$$

The requirement that the commutator be canonically normalized, $[\Phi, \Pi] = \delta^3(\vec{r} - \vec{r}')$, is equivalent to a completeness relation on the R_n functions:

$$\sum_n \frac{2}{B} \mu_n R_n^\dagger(\vec{r}) R_n(\vec{r}') = \delta^3(\vec{r} - \vec{r}')$$

Given that the R_n functions form a complete set, we can write down a related normalization condition,

$$\int \frac{2}{B} \mu_n R_n^\dagger(\vec{r}) R_n(\vec{r}) \sqrt{|g|} d^3 r = 1$$

Binding Energy Corrections to the mass M

$$\begin{aligned}
 \langle N | T_{00} | N \rangle &= f^2 \left[\frac{\mu_0^2 N R^2}{B f^2} + \frac{N R'^2}{A f^2} - m^2 [1 - J_0(X)] \right] \\
 &= f^2 \left[\frac{\mu_0^2 X^2}{4 B} + \frac{m^2 X'^2}{4 A} + \frac{m^2}{4} X^2 - \frac{m^2}{64} X^4 + \dots \right] \\
 &= f^2 m^2 \left[\frac{\epsilon_\mu^2}{4 B} \Delta^2 Y^2 + \frac{1}{4} \Delta^2 Y^2 + \frac{\Delta^4 Y'^2}{4 A} - \frac{\Delta^4 Y^4}{64} \right]
 \end{aligned}$$

Thus the mass is

$$\begin{aligned}
 M &= \int \langle N | T_{00} | N \rangle \sqrt{|g|} d^3 r \\
 &\approx \frac{f^2}{m \Delta} \pi \int \left[(1 - \Delta^2)(1 - \delta b) Y^2 + Y^2 + \frac{\Delta^2 Y'^2}{A} - \frac{\Delta^2 Y^4}{16} \right] \left[1 + \frac{\delta}{2}(a + b) \right] x^2 dx \\
 &= f^2 \int \left[Y^2 + \delta a Y^2 + \Delta^2 Y^2 + \frac{\Delta^2 Y'^2}{A} - \frac{\Delta^2 Y^4}{16} + \frac{\delta}{2}(a + b) Y^2 \right] x^2 dx
 \end{aligned}$$

Binding Energy Corrections to N

The particle number is

$$\begin{aligned}
 N &= \int \langle N | J^0 | N \rangle \sqrt{|g|} d^3 r \\
 &= \int \sqrt{\frac{A}{B}} 2 \mu_0 N R(r)^2 d^3 r \\
 &= \frac{f^2}{m^2 \Delta} 2 \pi \sqrt{1 - \Delta^2} \int \sqrt{\frac{1 + \delta a(x)}{1 + \delta b(x)}} Y(x)^2 x^2 dx \\
 &\approx \frac{f^2}{m^2 \Delta} 2 \pi \left[1 - \frac{\Delta^2}{2} \right] \int \left[1 + \frac{\delta}{2} (a - b) \right] Y(x)^2 x^2 dx \\
 &= \frac{f^2}{m^2 \Delta} 2 \pi \left[Y_0^2 + 2 Y_0 Y_1 - \frac{\Delta^2}{2} Y_0^2 + \frac{\delta}{2} (a - b) Y_0^2 \right] x^2 dx
 \end{aligned}$$

Leading Binding Energy Corrections

$$M = \frac{2\pi f^2}{m\Delta} \left[l_0 + 2l_1 + \frac{\delta}{2} l_a - \frac{\Delta^2}{2} l_0 + \frac{\Delta^2}{2} l_p - \frac{\Delta^2}{32} l_4 \right], \quad N = \frac{2\pi f^2}{m^2\Delta} \left[l_0 + 2l_1 + \frac{\delta}{2} l_a - \frac{\delta}{2} l_b - \frac{\Delta^2}{2} l_0 \right]$$

in terms of the integrals

$$l_0 = \int Y_0^2 x^2 dx$$

$$l_p = \int Y_0'^2 x^2 dx$$

$$l_4 = \int Y_0^4 x^2 dx$$

$$l_a = \int a Y_0^2 x^2 dx$$

$$l_b = \int b Y_0^2 x^2 dx$$

$$l_1 = \int Y_0 Y_1 x^2 dx$$

The binding energy, at leading order in δ, Δ^2 , is

$$E_B = M - mN = \frac{2\pi f^2}{m\Delta} \left[\frac{\delta}{2} l_b + \frac{\Delta^2}{2} l_p - \frac{\Delta^2}{32} l_4 \right]$$

Numerical Values

κ	M [kg]	R_{99} [km]	d [kg / m ³]	$\frac{E_B}{mN}$ [10^{-13}]
0.01	2.01×10^{18}	115	311	141
0.09	6.91×10^{18}	386	28.6	2.93
0.16	1.02×10^{19}	593	11.6	-3.24
0.25	1.27×10^{19}	854	4.85	-4.18
0.29	1.31×10^{19}	972	3.41	-3.99
0.34	1.33×10^{19}	1077	2.53	-3.71
0.38	1.32×10^{19}	1183	1.90	-3.39
0.64	1.20×10^{19}	1652	0.633	-2.25
1	1.03×10^{19}	2145	0.248	-1.49
4	5.56×10^{18}	4499	0.0146	-0.384
16	2.85×10^{18}	9062	0.000913	-0.109
100	1.15×10^{18}	22849	0.000023	$< 10^{-2}$

Table: Macroscopic parameters describing a dilute axion star: mass M , radius R_{99} , average density d , and reduced binding energy per particle E_B/mN , as a function of $\kappa = \delta/\Delta^2$. To set the numerical scale we have fixed the QCD parameters $m = 10^{-5}$ eV and $f = 6 \times 10^{11}$ GeV.

Computing the $3a_c \rightarrow a_p$ Decay Rate

We modify the axion field expansion to include a free axion term

$$\mathcal{A} = R(r)e^{-i\mu_0 t} a_0 + \int \frac{d^3 p}{\sqrt{2\mu_p}} e^{i\vec{p}\cdot\vec{r} - i\mu_p t} a_p(\vec{p}) + h.c.$$

This leads to the leading-order matrix element

$$\begin{aligned} \mathcal{M}_3 &\equiv \mathcal{M}[N \rightarrow (N-3) + 1 \text{ emitted}] \\ &= m^2 f^2 \int dt d^3 r \langle N-3, p | 1 - \cos\left(\frac{\mathcal{A}}{f}\right) | N \rangle \\ &= -i \frac{f}{m} \frac{1}{\sqrt{2\mu_p}} \int dt d^3 y J_3[Z(y)] e^{i\vec{p}\cdot\vec{r}} e^{i(3\mu_0 - \mu_p)t} \\ &= -i \frac{4\pi^2}{\sqrt{2\mu_p}} \frac{f}{p} \delta(3\mu_0 - \mu_p) \underbrace{\int_{-\infty}^{\infty} y \sin\left(\frac{p y}{m}\right) J_3[Z(y)] dy}_{I_3(p)} \end{aligned}$$

The Decay Rate at Weak Binding

Note that the dimensionless momentum $k = p/m$ of the ejected axion is sharply peaked for $E - m \ll m$

$$k_3 = \sqrt{9E^2/m^2 - 1} \approx \sqrt{8}$$

We find the decay rate for $3a_c \rightarrow a_p$ is

$$\begin{aligned} \Gamma_3 &= \frac{1}{T} \int \frac{d^3p}{(2\pi)^3 (2\mu_p)} |\mathcal{M}_3|^2 \\ &= \frac{2\pi f^2}{m k_3} |I_3(k_3)|^2 \end{aligned}$$

$$\begin{aligned} I_3(k) &= \int_{-\infty}^{\infty} y \sin\left(\frac{p y}{m}\right) J_3[Z(y)] dy \\ &= \frac{1}{\Delta^2} \int_{-\infty}^{\infty} x \sin\left(\frac{k x}{\Delta}\right) J_3[\Delta Y(x)] dx \\ &\stackrel{\Delta \ll 1}{\approx} \frac{\Delta}{48} \int_{-\infty}^{\infty} x \sin\left(\frac{k x}{\Delta}\right) Y(x)^3 dx \end{aligned}$$

In principle, we can use our solutions $Y(x)$ and integrate directly.
In practice, this is made difficult by the **rapidly oscillating *sin* term**

Contour Integration of $I_3(k)$

$$I_3(k_3) = \frac{\Delta}{48} \int_{-\infty}^{\infty} x \sin\left(\frac{k_3 x}{\Delta}\right) Y(x)^3 dx$$

Consider the contour integral instead:

- $Y(x)$ has no singularities along the real axis
- We show that the leading singular term is of the form $Y_s(x) = \frac{8 y_I}{x^2 + y_I^2}$ with $y_I \approx .603$
- Deforming the contour of integration until we reach $i y_I$, the contribution of this pole dominates the integral. The result is

$$I_3(k_3) = i \frac{32\pi y_I}{3\Delta} \exp\left(-\frac{k_3 y_I}{\Delta}\right)$$

Alternative Derivation: Spherical Waves

For our complete set of scattering states, we could have used

$$\phi_s(t, r) = \frac{1}{2\pi^2} \sum_{\ell=0}^{\infty} \sum_{\ell_z=-\ell}^{\ell} Y_{\ell, \ell_z}(\hat{r}) \int_0^{\infty} \frac{dp p}{2\mu_p} j_{\ell}(p r) e^{-i\mu_p t} a_{\ell, \ell_z}(p)$$

The spherical wave annihilation operators satisfy the commutation relation

$$[a_{\ell, \ell_z}(p), a_{\ell', \ell'_z}(p')] = (2\pi)^3 2\mu_p \delta(p - p') \delta_{\ell, \ell'} \delta_{\ell_z, \ell'_z}.$$

Note that the annihilation operators in the two bases are related as

$$a_{\ell, \ell_z}(p) = i^{\ell} p \int d\Omega_p Y_{\ell, \ell_z}^*(\hat{p}) a(\vec{p}),$$

which can also be inverted,

$$a(\vec{p}) = \frac{1}{p} \sum_{\ell=0}^{\infty} \sum_{\ell_z=-\ell}^{\ell} i^{-\ell} Y_{\ell, \ell_z}(\hat{p}) a_{\ell, \ell_z}(p).$$

Both sets of scattering states are *precisely equal*. One can be derived from the other by using the expansion of the exponential in spherical harmonics.

Alternative Derivation: Spherical Waves (2)

The transition matrix element in this basis has the form

$$\begin{aligned}\mathcal{M}_3^{sph} &= -i m^2 f \int dt d^3r J_3 \left(\frac{2\sqrt{N} R(r)}{f} \right) \langle 0 | \phi_s(t, r) | \vec{p} \rangle \\ &= -i m^2 f \int dt d^3r J_3 \left(\frac{2\sqrt{N} R(r)}{f} \right) \sqrt{4\pi} j_0(p r) e^{-i \mu_p t}\end{aligned}$$

Although this matrix element is different when using the spherical waves, the decay rate is calculated using a different integration over phase space,

$$\Gamma_3 = \frac{1}{T} \int \frac{1}{(2\pi)^3} \frac{dp}{2\mu_p} |\mathcal{M}_3^{sph}|^2$$

and the final answer is the same.

The Nonrelativistic Limit for Axions

Expand the axion field in the nonrelativistic limit as

$$\mathcal{A}(t, r) = \frac{1}{\sqrt{2m}} \left[e^{-imt} \psi(t, r) + e^{imt} \psi^*(t, r) \right].$$

In the axion potential, the n th term is proportional to the factor

$$\mathcal{A}^{2n} = \frac{{}^{2n}C_n}{(2m)^n} (\psi^* \psi)^n + \mathcal{O}(e^{\pm imt}),$$

where ${}^{2n}C_n$ are binomial coefficients. Dropping the rapidly oscillating pieces, we obtain

$$\begin{aligned} W(\psi) &= m^2 f^2 \left[1 - \cos \left(\frac{\mathcal{A}}{f} \right) \right] - \frac{m^2}{2} \mathcal{A}^2 \\ &\rightarrow m^2 f^2 \left[1 - \sum_{n=0}^{\infty} \frac{{}^{2n}C_n (-1)^n}{(2n)!} \left(\frac{\psi^* \psi}{2mf^2} \right)^n \right] - \frac{m}{2} \psi^* \psi \\ &= m^2 f^2 \left[1 - \frac{\psi^* \psi}{2mf^2} - J_0 \left(\sqrt{\frac{2\psi^* \psi}{mf^2}} \right) \right] \end{aligned}$$